

ENVIRONMENTAL EFFECTS ON Cu/SiO₂ AND Cu/Ti/SiO₂ THIN FILM ADHESION

N.I. TYMIAK, M. LI, A.A. VOLINSKY, Y. KATZ and W.W. GERBERICH
CEMS Department, University of Minnesota, MN 55455, tymiak@cems.umn.edu

ABSTRACT

For several microelectronics applications, Cu/dielectric adhesion is a key reliability issue. Either electroplating or local galvanic coupling under moist operating conditions may result in hydrogen induced interface weakening. The present study compared hydrogen effects on Cu/SiO₂ adhesion for sputter deposited films with and without Ti underlayers. Thin Cu and Cu/Ti films ranging from 80-3000 nm have been evaluated. Direct observations of the surface during electrolytic charging have shown no evidence of film/substrate debonding for Cu/Ti systems. In contrast, extensive delaminations have been observed for Cu films. Indentation testing immediately after charging indicated up to 100% decrease in the *practical adhesion* for Ti/Cu films. The observed effect resulted from a *true interfacial fracture energy* reduction from 4 to 2 J/m². Plastic energy dissipation was assumed unaffected as no yield stress changes were detected after charging. Even with the deleterious effect of hydrogen, adhesion strength of Cu/Ti films remained higher than that of non-charged Cu films.

INTRODUCTION

Environment may affect several aspects of thin film performance including its adhesion to a substrate, one of the key reliability issues in microelectronics. For Cu interconnects, both processing and operating conditions may involve electrolytically induced hydrogen, especially with electroplating becoming a major deposition route. Possible effects of hydrogen include the decrease of interfacial fracture energy, Γ_0 , and reduction of the plastic energy dissipation, Γ_p , via an increase of the Cu film yield stress. Both of the above would decrease the practical adhesion which can be characterized by the elastic strain energy release rate, G_{crit} , corresponding to the critical crack extension [1]:

$$G_{crit} = \Gamma_0 + \Gamma_p + \text{other forms of dissipation} \quad (1)$$

Compared with the other dissipation terms, Γ_p is dominant except, possibly, for very thin films and/or high interfacial roughness where frictional losses may be significant [2]. With no environment, plastic energy dissipation decreases with the decreasing film thickness [3-6] and becomes negligible in the limit of very thin films. Here, Γ_0 can be determined [1,4,5]. Up to an order of magnitude increase in both Γ_0 and practical adhesion could be accomplished by applying a nanoscale layer of Ti between Cu and SiO₂ [5,7,8]*. However, with the Ti interlayer, hydrogen trapping or even hydride formation along an interface may occur. Thus, it is not clear whether the presence of Ti will still be beneficial when hydrogen charging is involved. There were two objectives of the present research:

- Evaluate hydrogen effects on *practical* adhesion for Cu/SiO₂ and Cu/Ti/SiO₂ systems.
- Determine whether changes in practical adhesion (if any) result from a decrease in Γ_0 , a reduction of plastic energy dissipation or both.

MATERIALS AND PROCEDURES

Nanocrystalline thin Cu films with and without 10 nm Ti interlayers were RF sputtered onto oxidized Si wafers as described elsewhere [5]. A summary of film characteristics is given in

* The measured value $\Gamma_0^{Ti}_{Cu-SiO_2} = 4 \text{ J/m}^2$ [5] was higher than typical metal/metal interfacial surface energies but comparable to these for Al₂O₃ on W, Mo and Nb as obtained by contact angle measurements [9]. One possibility is that TiO₂ was formed prior to Cu deposition [5] and $\Gamma_0 = 4 \text{ J/m}^2$ corresponds to Cu/TiO₂ rather than a Cu/Ti interface. Higher surface roughness of Ti or TiO₂ as compared to that for SiO₂ can also be a reason for an observed increase in Γ_0 [5].

Table 1. Techniques utilized for film thickness and grain size determination as well as residual stress measurements and yield stress evaluation are detailed elsewhere [5].

Film thickness (nm)	Grain Size (nm)	σ_{vs} (GPa)
200	110	1.37
500	130	0.89
1000	150	0.84

Table 1. Cu film characteristics [4]

Hydrogen charging involved a 1M NaOH solution with a Pt electrode as an anode. Films ranging from 80 to 3000 nm have been evaluated qualitatively by surface monitoring during hydrogen charging. Additionally, AFM observations were carried out following charging. Attention was focused on the differences in hydrogen induced blister formation for Cu and Cu/Ti systems.

For a quantitative adhesion assessment, 200, 500 and 1000 nm thick Cu and Cu/Ti films have been examined under indentation loading. First, interfacial toughness was determined for non-charged samples. Next, films were tested immediately after ~80 sec of hydrogen charging at 60 mA/cm². Nanoindentation tests have been carried out with the 90° conical indenter of approximately 1 μm tip radius. Indentation loads of 50, 100, 200 300 and 400 mN were applied with the MMT, a device analogous to an IBM micromechanical tester described elsewhere [10].

Adhesion calculations were based on the Marshall and Evans analysis[11]. Here, critical strain energy release rate, G_{crit} , is defined as a function of the following parameters: E, Young's modulus; ν , Poisson's ratio; σ_R , residual stress in a film; R, delamination radius and V_0 , volume displaced by indentation. With the indentation depth exceeding film thickness, V_0 can be

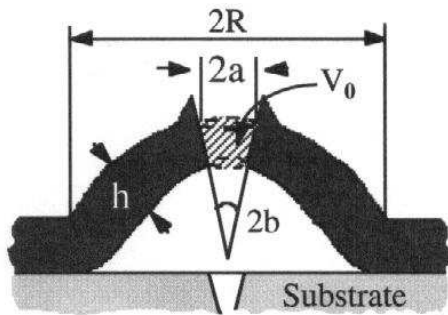


Figure 1. Schematic of an indentation induced delamination.

determined as a volume of a truncated cone with the height equal to the film thickness and a base equal to an indentation contact radius as shown in Fig. 1. Due to elastic recovery, an angle β is not equal to the indenter included angle. However, for a large contact radius, elastic recovery may be neglected. Delamination and contact radii as well as angles β have been evaluated from AFM scans of indentation induced blisters as shown in Fig. 2. Effects of radial cracking and indentation induced pile-up are discussed in the APPENDIX. Note that analysis does not require indentation curves.

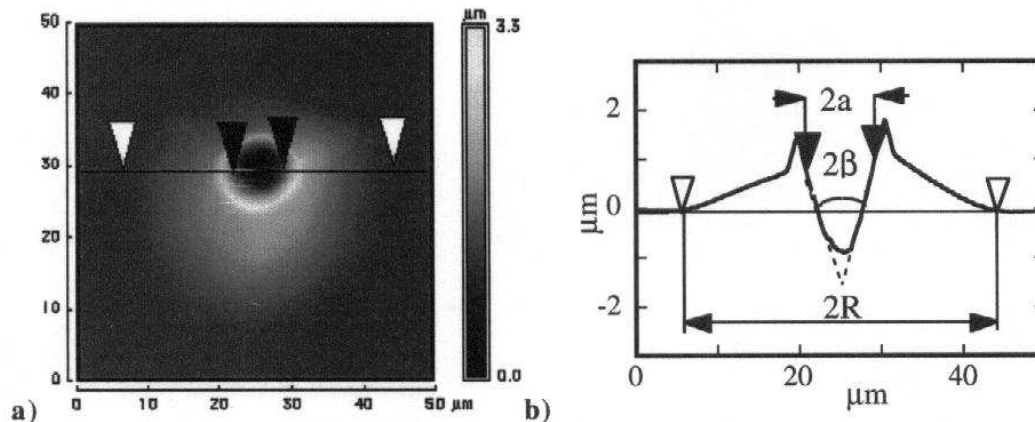


Figure 2. AFM measurements of delamination parameters. a) Blister image. b) Height profile

RESULTS AND DISCUSSION

Blisters Induced During Hydrogen Charging

A summary of Cu surface observations during and after charging is given in Table 2.

Cu film	without Ti	with Ti
80 nm 10 sec of charging.	Numerous macro-blisters Complete film destruction.	occasional micro-blisters
200-500 nm 80 sec of charging.	Few macro-blisters Partial film destruction	occasional micro-blisters
1-3 μm 1-2 min of charging	Film delaminates as a whole piece	no evident effect

Table 2. A summary of the film surface observations during hydrogen charging and following AFM evaluations.

While there was no evidence of film substrate debonding for Cu/Ti, an extensive blister formation followed by rupture or a complete film delamination occurred for Cu. Analysis of hydrogen induced blisters could possibly give a quantitative adhesion measures for Cu films providing the hydrogen fugacity is known. However, with no evident debonding, evaluation would not be possible for Cu/Ti films.

Indentation Induced Delamination.

Since for Cu films adhesion measurements would be hampered by charging induced interfacial fractures, only Cu/Ti films have been evaluated. Indentation curves for both charged and non-charged samples did not exhibit any irregularities which could be correlated to fracture events (interfacial, film or substrate) as shown in Fig. 3. Load/depth dependence was essentially the same for charged and non-charged films up to loads slightly above 100 mN. Then, indenter displacement increased at higher rates for charged films as seen from Fig. 3. These differences would be consistent with interfacial cracking initiation just above 100 mN and lower crack propagation resistance for charged samples. In a qualitative agreement with the above, for both charged and non-charged 200 and 500 nm thick films, delaminations were seen after 200 mN indents but no evident debonding was observed at 100 mN. Only partial delaminations were detected for a 1 μm noncharged film. In contrast, well defined blisters were seen on a charged film of the same thickness. For a given indentation load and film thickness, blisters were always larger for the charged films while contact radii were almost the same as those for non-charged films as evident from Fig. 4.

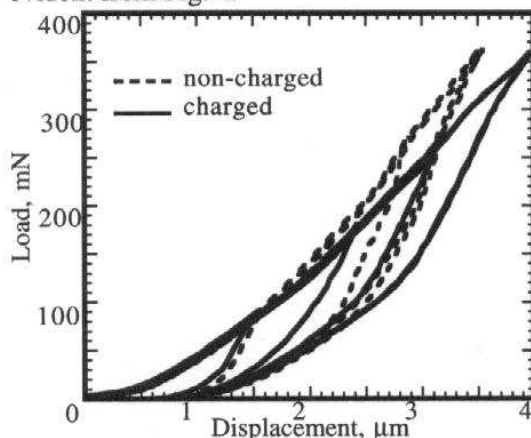


Figure 3. Indentation curves for 500 nm thick Ti/Cu films.

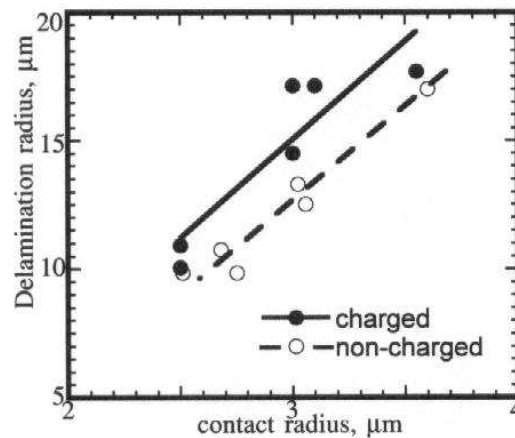
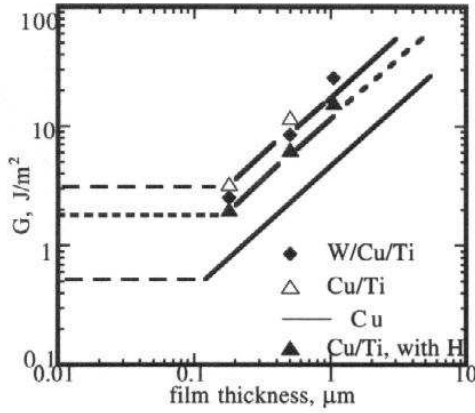


Figure 4 Delamination radii vs. contact radii for 200 nm thick films

Calculated strain energy release rates for charged and non-charged Ti/Cu films along with these for the non-charged Cu films are shown in Fig. 5. For comparison, data for W/Cu/Ti films determined with the superlayer technique [5] are also included. Overall, strain energy release rates for Ti/Cu films decrease after hydrogen charging but still remain higher than these for Cu only



even without hydrogen. Hydrogen induced reduction in the practical adhesion ranged from 60-100% increasing with increasing film thickness. To evaluate the significance of the plastic energy dissipation in the above effect, yield stress has been determined from nanoindentation into a 200 nm thick film charged at the identical conditions as one used for adhesion strength assessment. Independently, yield stress was determined for a non-charged sample.

Figure 5. Hydrogen effects on strain energy release rates for Cu/Ti/SiO₂ interfaces.

As measured from the above experiments, yield stress values were the same for both charged and non-charged samples. Thus, the availability of plastic energy dissipation was assumed unaffected by hydrogen and the observed adhesion deterioration was attributed to hydrogen induced interfacial fracture energy reduction. This can be evaluated based on the ratio of strain energy release rates with and without hydrogen as given by [12][†]:

$$\frac{G_1^i}{G_{1H}^i} = \exp\left\{\frac{E(\Gamma_{\text{Cu-SiO}_2}^{\text{Ti}} - \Gamma_{\text{Cu-SiO}_2}^{\text{Ti-H}})}{\pi^2 \alpha' \sigma_{ys}}\right\} \quad (2)$$

Here, E is film modulus; α' , a constant specific for a given film/substrate system; σ_{ys} , the Cu film yield stress. The interfacial fracture energy, $\Gamma_{\text{Cu-SiO}_2}^{\text{Ti}}$ accounts for the Dupre' energy (true surface energy), $\gamma_{\text{Cu-SiO}_2}^{\text{Ti}}$ and microstructural contributions such as mechanical interlocking and/or defects along an interface. The values of α' and E used herein were 40 J/m² and 120 GPa respectively. A parameter α' was determined based on the experimental data for Cu/SiO₂ and Cu/Ti/SiO₂ interfaces [12]. Values of σ_{ys} as obtained with the nanoindentation [4] are given in the Table 1. For a 500 nm thick film, the ratio of 11.8/6.3 gave a reduction of $\Gamma_{\text{Cu-SiO}_2}^{\text{Ti}}$ from 4 J/m² [5] down to 2.2 J/m². Similarly, data for 200 nm and 1000 nm thick Cu films yielded reduced values of 1.8 and 2 J/m² respectively. These results suggest that hydrogen segregated along the interface and reduced interfacial fracture energy from 4 down to approximately 2.2 J/m². To determine the interface along which fracture occurs, scotch tape was used to remove indentation induced blisters. In qualitative agreement with the hydrogen induced interface weakening, only part of the film exposed to charging delaminated. According to Auger electron depth profiling failure occurred either along the Cu/Ti or Cu/TiO₂ interface. Differentiation between these two was not possible as separation along the Ti/Cu interface would necessarily involve oxidation following film removal. Hydrogen induced changes in surface energies of both Cu and Ti as well as Cu/Ti interfacial energy may contribute towards changes in interfacial surface energy:

$$\gamma_{\text{Cu-SiO}_2}^{\text{Ti}} = \gamma_{\text{Cu}} + \gamma_{\text{Ti}} - \gamma_{\text{Ti/Cu}} \quad (3)$$

Here, γ_{Cu} and γ_{Ti} are surface energies for Cu and Ti respectively and $\gamma_{\text{Cu/Ti}}$ is an interfacial energy. Among possible mechanisms accounting for the interfacial fracture energy degradation would also be microstructural changes such as hydrogen induced microvoiding, microcracking and hydride formation. More extensive examination of fracture surfaces and a precise composition analysis would be needed as well as evaluation of hydrogen effects on surface energies of Cu and

[†] This relationship is derived based on the relation between the *applied* stress intensity and the *local* crack tip stress intensity as affected by dislocation shielding [13]. With the local stress intensity related to the interfacial fracture energy and applied stress intensity expressed via strain energy release rate, Eq.2 can be obtained as detailed elsewhere [12]. The exact application of the discrete dislocation model at the crack tip to thin film material characterization have been elaborated elsewhere [12,13].

Ti. Also, adhesion evaluation at different times after hydrogen charging would provide an insight into possible time dependent effects. Factors which might affect adhesion calculations are discussed in the APPENDIX.

SUMMARY

Effects of electrolytic hydrogen charging in 1M NaOH have been evaluated for a Cu/SiO₂ interface with and without a nanoscale Ti interlayer. Presence of a Ti interlayer has been shown to prevent a Cu film rupture and/or a complete delamination during charging. However, up to 100 % reduction of the practical work of adhesion was observed in Cu/Ti/SiO₂ films as revealed by indentation testing immediately after charging. The effect increased with the increasing Cu film thickness. With no changes in the yield stress, plastic energy dissipation was assumed unaffected. Thus, adhesion degradation was attributed to the reduction of an interfacial fracture energy. An estimated decrease was from 4 down to 2.2 J/m². Even with the above deleterious effect of hydrogen, adhesion strength of the Cu/Ti interface was still higher than that for the Cu/SiO₂ interface without charging.

ACKNOWLEDGMENTS

The authors would like to acknowledge support for this work under grant NSF/CDR-8721551 and under DOE contract DE-FG02/96ER45574. In addition, N.I.T. wishes to thank Prof. J.V.R.Heberlein and Prof. S.L.Girshick for support under NSF DMI-9871863. The assistance of Dr. J.C.Nelson and D. Caldwell is also gratefully appreciated.

REFERENCES

1. Y.Weï and J. Hutchinson, *J.Mech. Phys. Solids*, **45**, p. 1137, (1997).
2. R.G. Stringfellow and L.B. Freund, *Int.J.Solids Structures*, **30**, p. 1379 (1993).
3. A.Bagchi and A.G. Evans, *Thin Solid Films*, **286**, p.203 (1986).
4. N.I. Tymiak, A.A. Volinsky, M.D. Kriese, S.A. Downs and W.W. Gerberich, submitted to *Met. Trans.*, (1999).
5. A.A. Volinsky, N.I. Tymiak, M.D. Kriese, W.W. Gerberich and J.W. Hutchinson, accepted for publication in *MRS Proceedings*, Symposium M, Fall 1998.
6. W.W. Gerberich, D.E. Kramer, N.I. Tymiak, A.A. Volinsky, D.F. Bahr and M.D. Kriese, accepted for publication in *Acta Metall. Mater.* (1999).
7. S.W. Russell, S.A. Raflaski, R.L. Spreitzer, J. Li, M. Moïnpour, F. Moghadam, T.L. Alford, *Thin Solid Films* **262**, p. 154 (1995).
8. M.D.Kriese, N.R.Moody and W.W.Gerberich, accepted for publication in *Acta Metall. Mater.*, (1999).
9. V.P. Elyutin, B.S. Mitin and E.F. Grits, *Inorganic Materials*, **10**, p. 723 (1974).
10. T.W. Wu, *J.Mater. Res.*, **6**, p.407, (1991).
11. D.B.Marshall and A.G.Evans, *J.Appl.Phys.*, **56**, p. 2632 (1984).
12. Y. Katz, N. Tymiak and W.W.Gerberich, An invited paper for *Recent Advances in the Engineering Aspects of Hydrogen Embrittlement of the Engng.Fract.Mech*, (1999).
13. H.Huang and W.W. Gerberich, *Acta. Metall. Mater.*, **42**, p. 639, (1994).

APPENDIX

Qualitatively, detrimental effect of hydrogen is apparent from larger delaminations for equal contact radii. However, quantitative measurements for charged and non-charged films may be affected differently by factors such as indentation pile-up, radial and substrate cracking.

Radial cracking

Total energy of a circular delamination with radial cracks can be expressed as follows:

$$U = U(R) + 2A\gamma_{\text{interface}} + 2S\gamma_{\text{film}} + U_1(R, c). \quad (\text{A.1})$$

Here, $U(R)$ is the energy of a delamination with the absence of radial cracking; $U_1(R,c)$, energy resulting from a stress state due to radial cracking; c , radial crack length, S and A are radial and interfacial crack areas respectively. For a critical growth of an interfacial crack, $dU/dA=0$

$$\partial U/\partial A = \partial U(R)/\partial A + \Gamma_0 + 2\gamma_{\text{film}} \partial S/\partial A + \partial U_1(R,c)/\partial A = 0. \quad (\text{A.2})$$

With the strain energy release rate without radial cracking being $G(R) = -dU(R)/dA$, the strain energy release rate for a radially cracked film, $G(R,c)$ becomes:

$$G(R,c) = G(R) - \partial U_1(R,c)/\partial A - 2\gamma_{\text{film}} \partial S/\partial A. \quad (\text{A.3})$$

With radial cracking driven by an indenter induced circumferential tension, stress at the radial crack tip will decrease with increasing compressive stresses at the delamination edge. For a given indenter penetration, these decrease with increasing A . Thus, $\partial U_1(R,c)/\partial A$ and $\partial S/\partial A > 0$ results in $G(R,c) < G(R)$. Consequently, radial cracking will result in *overestimated* G values. The physical picture is that as the radial cracks form, the stored elastic energy available for delamination decreases. This results in a decreased delamination radius which provides an overprediction of G . There was no difference in radial cracking extent for charged and non-charged films. Thus, for charged films with the larger R and the same values of a and c , an overestimate will be higher. Consequently, hydrogen effects are likely to be underestimated.

Pile-up.

With the significant amount of pile-up, a correction should be made by subtracting a pile up volume from a calculated value of V_0 . Pile-up heights and residual contact radii changes for the loads above a delamination threshold have been evaluated. While residual contact radii continued to increase with increasing load, pile-up heights remained almost unchanged as compared to indentations just below a delamination load.

For the loads just higher than delamination load, neglecting a pile-up effect will give the highest *overestimate* in G values. With increasing load, as indentation volume increases relative to a pile-up volume, any error will decrease. With the similar pile-up characteristics for charged and non-charged films observed experimentally, effect will be the same for both.

Substrate cracking

Substrate cracking could possibly initiate and/or contribute towards discontinuities in interfacial cracking. Fig. A.1 shows partially removed indentation blisters for 500 nm charged and non-charged Cu/Ti films indented at 400 mN peak load. For both of the above, substrate cracks are present. There could be a difference in the substrate cracking effects on the interfacial crack initiation and propagation for charged and non-charged samples. However, quantitatively, the only difference is an extent of delamination which will reflect the magnitude of hydrogen effect.

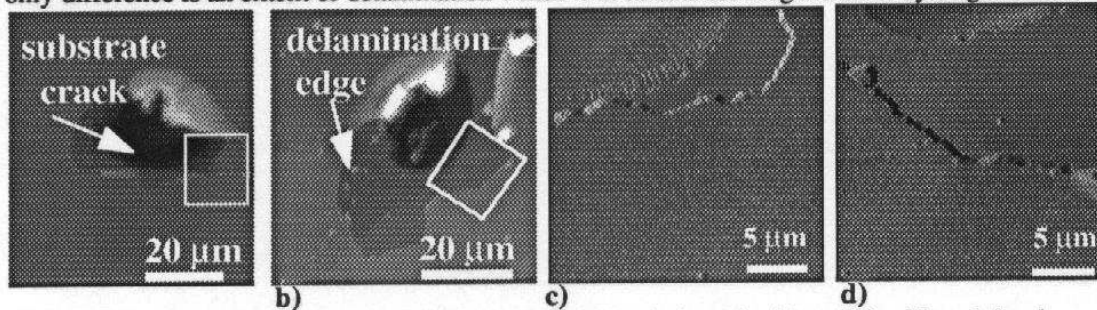


Figure A.1. Substrate cracking in a 200 nm Cu/Ti film indented with a 400 mN peak load. a) non-charged sample; b) charged sample; c) and d) show magnified areas of a) and b) respectively.

In summary, it may be suggested that all the factors considered may affect adhesion measurements. However, their effects will be similar for both charged and non-charged films except for radial cracking which might result in an underestimate of hydrogen effects.